Building a Globally Optimized Computational Intelligent Image Processing Algorithm for On-Site Inference of Nitrogen in Plants

Susanto B. Sulistyo
Newcastle University

W.L. Woo
Newcastle University

S.S. Dlay
Newcastle University

Bin Gao
University of Electronic Science and Technology of China

Estimating nutrient content in plants is a crucial task in the application of precision farming. This work will be more challenging if it is conducted nondestructively based on plant images captured in the field due to the variation of lighting conditions. This paper proposes a computational intelligence image processing to analyze nitrogen status in wheat plants. We developed an ensemble of deep learning multilayer perceptron-using committee machines for color normalization and image segmentation. This paper also focuses on building a genetic-algorithm-based global optimization to fine tune the color normalization and nitrogen estimation results. We discovered that the proposed method can successfully normalize plant images by reducing color variabilities compared to other color normalization techniques. Furthermore, this algorithm is able to enhance the nitrogen estimation results compared to other non-global optimization methods as well as the most renowned SPAD meter based nitrogen measurement.

Precision farming (PF), also known as site-specific crop management, has been a popular issue in agriculture recently. Furthermore, with the support of recent technologies in sensors and computers, the PF technology will be vastly beneficial to future farming.[1] This technology aims to boost crop productivity with fewer production costs and small negative impacts to surroundings. In order to support this technology, it is important to estimate the nitrogen status of plants to improve the efficiency of fertilizer use and prevent over-fertilizing that will harm the environment.

During recent years, image-based analysis to estimate nutrient content in plants has been extensively conducted by numerous researchers due to the rapid developments of vision sensing and computational systems. However, most of the image-based nutrient estimation approaches are conducted in a controlled environment with artificial lighting systems.[2] Such methods are impractical and time-consuming, and they require additional equipment. It is a challenging task to estimate nutrient content in plants based on the leaf images captured in the field under sunlight due to the variation of light intensities. The main problem is how to normalize the plant images by reducing color variability so that the images become more comparable among each other and the nutrient estimation results will be more reliable.

In our earlier work,[3] an MLP fusion based color normalization was developed to tackle the variation of sunlight intensities in wheat plant images. However, the work still suffers from several drawbacks where the neural network architecture has not been globally optimized leading to inability to distinguish weeds from wheat plants under the same sunlight intensity. Additionally, the other problem of on-field nitrogen content prediction is how to remove complex background, for instance weeds, stones, soils, and dry leaves, from wheat leaves as the region of interests.

In the current paper, we are focusing on applying genetic algorithm (GA) to establish further fine tuning of the color normalization based on the results of nitrogen content prediction. We also investigate multi-order statistical feature extraction of the normalized plant images and apply them in order to estimate nitrogen content in wheat plants. To achieve these research goals, we developed a new method to fuse deep learning multilayer perceptron (DL-MLP) by means of committee machines for color normalization and image segmentation, and to globally optimize the overall system architecture for high performance of color normalization and nitrogen status estimation using GA.

Many deep learning methods have been developed by several researchers, such as convolutional neural network (CNN)[4] and recurrent neural network (RNN).[5] Basically, CNN embeds a set of filters into the model, and these filters are typically invariant to certain shapes, orientations, and sizes. As such, CNN is useful for extracting independent features in images. These features correspond to some common observed patterns (i.e. basis representations) in the images. However, these are not the final output of our research. Instead, we developed an approach for extracting several statistical features at various orders from the plant images. Our main goal is to build a robust statistical model for prediction, rather than just recognizing the images. Furthermore, RNN is not suitable for our dataset since RNN imposes a temporal feedback constraint into the prediction model, which in our problem is not required and in fact may produce bias.

FARM EXPERIMENTAL AND CHLOROPHYLL METER BASED NITROGEN ANALYSIS

We conducted a farm experiment in Nafferton Farm, Northumberland, UK to produce and record nitrogen level variations in wheat plants. Three variations of nitrogen fertilizer amounts, i.e. 0 kg/ha (N1), 85 kg/ha (N2), 170 kg/ha (N3) of NH_4NO_3, were applied to field plots with each treatment replicated four times. The nutrient data was collected one week prior to fertilizing as well as two and four weeks after fertilizing.[6] We also measured nitrogen content using a chlorophyll meter (Minolta SPAD-502) as a comparison. A SPAD meter is a non-destructive device to determine chlorophyll content in a leaf by measuring the absorbance and transmittance of lights with two different wavelengths, i.e. red and infrared lights with peak wavelengths of 650 nm (I_{650}) and 940 nm (I_{940}), respectively, through the leaf.

COMBUSTION METHOD BASED ACTUAL NITROGEN MEASUREMENT

The actual nitrogen content was measured using an Elementar Vario Macro Cube. The measurement procedure comprises leaf sample collection, oven drying, pulverization, and sample burning in the Cube device with a certain amount of oxygen. The nitrogen element was then analyzed and a percentage figure subsequently obtained.

PROPOSED COMPUTATIONAL IMAGE-BASED NITROGEN STATUS ANALYSIS

In general, this proposed method can be split into five major steps, as shown in Figure 1, i.e. (i) image acquisition, (ii) color normalization training using an ensemble of deep learning multilayer perceptron (DL-MLP), (iii) image segmentation and feature extraction, (iv) nitrogen estimation, and (v) GA-based global optimization. All computational algorithms in this research, including neural networks, image processing, and genetic algorithms, were developed using MATLAB R2012 and the analyses were performed by means of a desktop PC with 3.2 GHz Intel Core i5 processor and 8 GB of RAM. Furthermore, the details of each particular work will be described in the following sections.

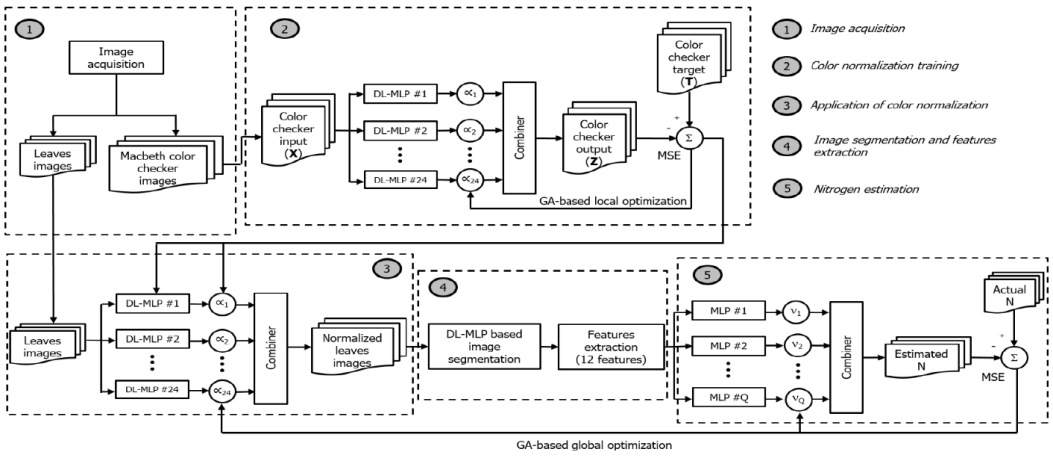

Figure 1. Genetically-enabled ensemble DL-MLP for on-field nitrogen status analysis in plants.

Image Acquisition

In this research, two types of images were acquired in the field with variations of sunlight intensities, i.e. Macbeth color checker and wheat plant images. The images of the Macbeth color checker and wheat plant were captured under sunlight using a common digital still camera. The image acquisition adopted the method used in our preceding research.[3] There were 7872 RGB color samples from the Macbeth color checker for color normalization and 360 wheat plant images for nutrient estimation.

Color Normalization Training and Its Application to Wheat Plant Images

In this step, we performed a color normalization using an ensemble deep learning multilayer perceptron (DL-MLP) and then locally optimized the results by genetic algorithm using the Macbeth color checker datasets. The developed color normalization aims to reduce color variability

produced by different light intensities. As shown in Figure 1, the RGB information of the Macbeth color checker was initially trained by using 24 DL-MLPs and combined using Macbeth color checker by both simple and weighted averaging methods.

In order to attain a better generalization performance, a deep learning MLP is required to extract more abstract and accurate information than can be obtained from a shallow one. Each DL-MLP consisted of three hidden layers and three units of both input and output layers, which represented red, green and blue color channels from the Macbeth color checker. A DL-MLP uses a series of many layers (usually more than one hidden layer) of nonlinear processing units. Each consecutive layer uses the output from the previous one as input. Suppose that there is a DL-MLP with L hidden layers, the layer input activation for $k > 0$ with $\mathbf{h}^{(0)}(\mathbf{x}) = \mathbf{x}$ can be expressed as:

$$\mathrm{a}^{(\mathrm{k})}(\mathrm{x}) = \mathrm{b}^{(\mathrm{k})} + \mathrm{W}^{(\mathrm{k})}\mathrm{h}^{(\mathrm{k}\text{-}1)}(\mathrm{x}) \tag{1}$$

where **a** is layer activation, **b** is offset vector (bias), **W** is weight matrix, and **h** is hidden layer output.

The hidden layer activation (k from 1 to L) and output layer activation ($k = L + 1$), thus, can be calculated as:

$$\mathbf{h}^{(\mathrm{k})}(\mathbf{x}) = \mathrm{g}\left(\mathbf{a}^{(\mathrm{k})}(\mathbf{x})\right) \tag{2}$$

and

$$\mathbf{h}^{(\mathrm{L}+1)}(\mathbf{x}) = \mathrm{o}\left(\mathbf{a}^{(\mathrm{L}+1)}(\mathbf{x})\right) = \mathbf{f}(\mathbf{x}) \tag{3}$$

respectively, where $\mathrm{g}(\cdot)$ and $\mathrm{o}(\cdot)$ are the sigmoid activation function.

In the developed DL-MLP, each hidden layer is initially pre-trained in an unsupervised way using an autoencoder. After pre-training all the hidden layers, each weight and bias value is subsequently fine-tuned by supervised learning using backpropagation method. Basically, an autoencoder is a feedforward neural network that will transform the input into a more dense representation and rebuild the input with the learned representation.[7]

After autoencoding the first layer, the pre-training process continues to the next hidden layer with the same method as previously described until the last hidden layer. Once all hidden layers are pre-trained, the next step is as follows:

- Add output layer
- Initialize $\mathbf{W}^{(L+1)}$ and $\mathbf{b}^{(L+1)}$ randomly as usual
- Train the whole network using supervised learning with a backpropagation error algorithm. All networks' weights are then adjusted for the supervised task.

After training each DL-MLP, the next step is combining all 24 DL-MLPs into a single network system using committee machines. By using this combination, the output value **Z** (see Figure 1) can be achieved by averaging the output **Y**, as follows:

$$Z = a \cdot Y = [\propto_1, \propto_2, \propto_3, \ldots, \propto_{24}] \cdot [Y_1, Y_2, Y_3, \ldots, Y_{24}]^T \tag{4}$$

The combination of several neural networks by a committee machine is able to considerably improve the estimation results. Suppose that there are Q expert systems to approximate a target vector T. Each expert has output vector O_i and error e_i,

$$\mathrm{O_i} = \mathrm{T} + \mathrm{e_i} \tag{5}$$

Thus, the sum of the squared error for the i-th expert y_i is

$$E_i = \xi\left[(O_i - T)^2\right] = \xi\left[e_i^2\right] \tag{6}$$

where $\xi[\cdot]$ denotes the statistical expectation.

The average error of each expert system (E_{ave}) is then

$$E_{ave} = \frac{1}{Q}\sum_{i=1}^{Q} E_i = \frac{1}{Q}\sum_{i=1}^{Q} \xi[e_i^2] \tag{7}$$

In other words, by using a committee machine, the output value Y can be achieved by simply averaging the output vector O_i, as follows:

$$Y = \frac{1}{Q}\sum_{i=1}^{Q} O_i \tag{8}$$

Thus, the squared error of the committee machine (E_{COM}) is

$$\begin{aligned} E_{COM} &= \xi\left[(Y-T)^2\right] \\ E_{COM} &= \xi\left[\left(\frac{1}{Q}\sum_{i=1}^{Q} O_i - T\right)^2\right] = \xi\left[\left(\frac{1}{Q}\sum_{i=1}^{Q} e_i\right)^2\right] \end{aligned} \tag{9}$$

But, by considering Cauchy's inequality, Eq. (10) and (12) is as follows:

$$\xi\left[\left(\frac{1}{Q}\sum_{i=1}^{Q} e_i\right)^2\right] \le \frac{1}{Q}\sum_{i=1}^{Q} \xi\left[e_i^2\right] \tag{10}$$

Thus, we have

$$E_{COM} \le E_{ave} \tag{11}$$

which indicates that the committee machine gives more accurate and reliable estimations than any one of the individual neural network.

We used two types of combiner, i.e. simple and weighted averaging methods. The simple averaging method indicates that each DL-MLP has the same weight, $\propto_k$, to produce the new output, **Z**. We also investigated the possibility that each DL-MLP has a different weight, which was optimized locally using a genetic algorithm, as expressed in the following:

$$Z = \sum_{k=1}^{24} (\propto_k \times Y_k) \tag{12}$$

with

$$\sum_{k=1}^{24} \propto_k = I \tag{13}$$

Once the color normalization is accomplished, the next step is to apply the developed neural network and the matrix α to normalize wheat plant images. The wheat plant image has a dimension of 448×336 pixels. Through this developed color adjusting system, each pixel of a plant image which was acquired under various light intensities is transformed to the equivalent pixel of the image under the standard light intensity, i.e. 50 Klux.

Image Segmentation and Feature Extraction

Image segmentation was conducted to remove any non-leaf images, such as soil, stones, weeds, dried and semi-dried leaves, and to keep the leaf images as the region of interest. We used a DL-MLP for image segmentation to distinguish the wheat leaves from other undesired parts. We established a dataset of 4,800 samples of RGB color and binary values (0 or 1) as the input and target values, respectively. The dataset was achieved from 24 images, in which 100 pixels in the leaf region and 100 pixels in other parts of the region were selected manually from each image. The structure of the neural network in this step is similar to the single DL-MLP used for color normalization. The output layer had only one unit, which signifies whether each pixel is a part of a leaf or not. The output value of the network was equal to 1 if the corresponding pixel was a part of a leaf, otherwise, the value was 0. We used three hidden layers which were initially pre-

trained unsupervised using the autoencoder method. The sigmoid activation function was used for both hidden and output layers.

In the color segmented images, noise is minimized before extracting image features. Furthermore, weeds were present in most of the plant images, which needed to be removed from the segmented images, as they affect the color information of the wheat leaves. To unravel this problem, we developed an algorithm to remove unwanted images by selecting the largest part of the leaves which has the highest number of object pixels.

Once the image segmentation is accomplished, several features of the segmented images were subsequently extracted. We extracted four types of statistical color moments of each RGB color channel, namely mean, variance, skewness, and normalized kurtosis, as these features can represent color distributions of an image. Additionally, the mathematical expressions of the features can be written as follows:

$$mean = \mu^{(c)} = E\left(x^{(c)}\right) = \frac{1}{P}\sum_{p=1}^{P} x_i^{(c)} \tag{14}$$

$$\text{variance} = \text{var}^{(c)} = E\left[\left(x^{(c)} - \mu^{(c)}\right)^2\right] = \frac{1}{P}\sum_{p=1}^{P}\left(x_i^{(c)} - \mu^{(c)}\right)^2 \tag{15}$$

$$\text{skewness} = skew(c) = \frac{E\left(x^{(c)} - \mu^{(c)}\right)^3}{\left(E\left[\left(x^{(c)} - \mu^{(c)}\right)^2\right]\right)^{3/2}} \tag{16}$$

$$\text{normalized kurtosis} = normkurt^{(c)} = \frac{E\left[\left(x^{(c)} - \mu^{(c)}\right)^4\right]}{\left(E\left[\left(x^{(c)} - \mu^{(c)}\right)^2\right]\right)^2} - 3 \tag{17}$$

Where c refers to each color channel (red, green, and blue) and P is the number of object pixels.

Nitrogen Content Estimation

We developed a combination of several standard MLPs with different hidden layer nodes using a committee machine to estimate nitrogen content. Each neural network had twelve nodes of input layer which correspond to the statistical moment features of red, green, and blue color and one node of output layer that represents the estimated nitrogen amount. Additionally, the initial number of hidden layer nodes was set to 18 nodes. To determine the initial number of hidden layer nodes, we modified the formula developed by Ward System Group[8] as follows:

$$Lh = \tau\left(\frac{Li + Lo}{2}\right) + \left(n_p\right)^{0.5} \tag{18}$$

Where Lh, Li, and Lo are the number of hidden, input, and output layer nodes, respectively, while n_p is the number of input patterns in the training set (number of training samples), and τ is a constant $(0 < \tau < 1)$. After conducting many experiments by trial and error, $\tau = 0.25$ is chosen.

From this initial hidden nodes number, we generated a number of new neural networks with various hidden layer nodes. The numbers of hidden layer nodes with regards to these new neural networks were produced using the following formula:

$$Lh_{new} = f \times Lh_{init} \tag{19}$$

where Lh_{new} and Lh_{init} are the number of hidden layer nodes of the new neural network and the initial neural network, respectively, and f is the multiplication factor. In this paper, we used $f = 2, 3, \ldots, 7$. Basically, the f number could be any number. The purpose of this multiplication factor is to produce new neural networks with different hidden nodes. In this research, f also denotes the number of neural networks combined by a committee machine (up to 7 neural networks).

We estimated the nitrogen amount by applying a committee machine. In a committee machine, a number of neural networks are combined to solve a complex estimation task. The fusion of these neural networks can improve the estimation results significantly compared to results attained by any single one of the networks.[9] We employed both simple and weighted averaging methods as the combiner of Q neural networks. The estimated nitrogen amount was obtained by the following formula:

$$N' = \sum_{q=1}^{Q} \left(v_q \times N_q \right) \text{ with } \sum_{q=1}^{Q} v_q = 1 \tag{20}$$

where N' is the estimated nitrogen content, v is the network's weight, and N_q is the output of a single network. In the committee machine with a simple averaging method, the value of v_q with $q = 1,2,\ldots,Q$ is the same for all networks. In contrast, the value of v_q is different for each neural network in the committee machine with a weighted averaging method.

Global Network Optimization

The final step of this research was to globally optimize the combiner weights, i.e. matrix α $\left(\alpha = \left[\propto_1, \propto_2, \propto_3, \cdots, \propto_{24}\right]\right)$ and matrix v $\left(v = \left[v_1, v_2, \ldots, v_Q\right]\right)$, in the color normalization and nitrogen estimation steps, respectively, based on the nutrient estimation error using a genetic algorithm (see Figure 1). Basically, a genetic algorithm encompasses a population with a certain number of individuals. Each individual in a population has the possibility of being the solution to the optimization problem. Hence, by applying selection, crossover, and mutation among individuals, a new generation is produced. This process is repeated several times until a new individual provides the most appropriate solution for the problem.

Two sequential GAs have been developed to achieve the best estimation results. The first GA was to optimize the matrix α in the color normalization, while the second was a GA to optimize the matrix v in the nitrogen estimation step. Based on our experiments, the developed DL-MLP fusion can be optimized using genetic algorithms with the following steps:

1. Define fitness function
    a. In this section, the fitness function of the developed genetic algorithm was to minimize the MSE between the actual $\left(N^*\right)$ and the estimated nitrogen content $\left(N'\right)$ of S samples.

$$\underset{\propto}{\operatorname{argmin}} \frac{1}{S} \sum_{s} \left(N_s^* - N_s' \right)^2$$

for color normalization step

$$\underset{v}{\operatorname{argmin}} \frac{1}{S} \sum_{s} \left(N_s^* - N_s' \right)^2$$

for nitrogen estimation step

2. Determine initial population of chromosomes (P_0)
    a. We set the initial population size of this genetic algorithm to 1000 chromosomes (individuals) for both steps. These initial chromosomes performed as the first generation.

$$P_0 = 1000$$

3. Encoding
    a. Encoding is expressing each chromosome in the population by the binary strings of 0s and 1s.

b. In the color normalization step, the $\alpha = [\propto_1, \propto_2, \propto_3, \cdots, \propto_{24}]$ matrix has a dimension of 3 × 72 and every element of the matrix $\propto_k$ was expressed by a 10-bit string of binary numbers (0s and 1s). Likewise, in the nitrogen estimation step, each chromosome (individual) referred to Q neural networks' weights $\nu = \nu_1, \nu_2, \ldots, \nu_Q$. Each chromosome, therefore, was represented by Q × 10 bit strings.

4. Boundary conditions

a. In both steps, we defined boundary conditions so that every element in the matrix α and matrix ν has a positive value. In particular, the boundary of each element of matrix $\propto_k$, i.e. $a_{k,ij}$ with i, j = 1,2,3, was set as follows:

If $i = j$ then
$a_{k,ij} \in [0,1]$
Else
$a_{k,ij} = 0$

a. Thus, each matrix $\propto_k$ has a structure as follows:

$$\propto_k = \begin{bmatrix} a_{k,11} & 0 & 0 \\ 0 & a_{k,22} & 0 \\ 0 & 0 & a_{k,33} \end{bmatrix} \quad (21)$$

With k = 1,2,3,…,24.

5. Reproduce next generations ($P_1, P_2, P_3, \ldots$) by processing selection, cross-over and mutation operators

a. In the beginning, each chromosome in the first generation (P_0) was tested by the fitness function to figure out how well it solves the optimization problem.

b. The selection operator attempts to give "a pressure" to the population as the same as similar to natural selection. Chromosomes (individuals) with better performance, or fitter, will be kept to the next generations. Otherwise, they will be wiped out. In cross-over, two chromosomes exchange some bits of the same section with one another to create two off-spring, while mutation turns over bits in a chromosome (a 0 to a 1 and vice versa).

c. The existence of mutation depends on the probability of mutation (ρ) set in the algorithm as well as a random number given by the computer (ω). In this step, we set the ρ value was 0.005. The mutation operator was defined as follows:

$$\text{mutation} = \begin{cases} 1 \text{ (occurs) if } \rho \geq \omega \\ 0 \text{ (not occur) if } \rho < \omega \end{cases} \quad (22)$$

6. Repeat the selection, crossover, and mutation processes until the best chromosome is found.

RESULTS AND DISCUSSION

In this study, we established three schemes of nitrogen status analysis based on the combiner type and the application of global optimization. In the first scheme, we used a simple average combiner for color normalization and nitrogen estimation. Meanwhile, the second scheme used a

GA-based weighted average combiner for color normalization with local-optimized matrix α and a simple average for nitrogen estimation. In these first two schemes, we did not apply global optimization. In the last scheme, GA-based global optimization was applied to color normalization and nitrogen estimation to globally optimize matrix α and matrix ν, respectively.

To determine the effectiveness of the DL-MLP fusion for color normalization, we compare the proposed approach with various machine learning algorithms, i.e. gray world (GW), white patch (WP), linear regression (LR), single MLP and MLPs fusion. Based on our experiments, the proposed DL-MLP is superior to other color normalization methods in terms of Euclidean error (ΔE_{RGB}) which measures the color difference of output and target RGB values. The ΔE_{RGB} of GW, WP, LR, MLP, and MLPs fusion are 22.30, 13.74, 11.03, 4.85, and 4.10, respectively, while the ΔE_{RGB} of the proposed DL-MLP method is 3.67.

The developed DL-MLP based color normalization using 24-patch Macbeth color checker can be applied to normalize plant images as well as to reduce color variability due to different sunlight intensities. In Figure 2, we show some examples of average RGB standard deviation which were taken from 30 images from three field plots. As seen in the figure, without color normalization, the color variability of plant images is very high as indicated by the average standard deviation of RGB color. It means that various sunlight intensities have considerable effects on the color of wheat plant images. Such images cannot be used directly for nutrient estimation since they are not comparable. Theoretically, all plants from the same plot should have similar color values since they are subject to the same fertilizer treatment. The color of the wheat leaves is considerably influenced by the nutrient amounts in the leaves, especially nitrogen.

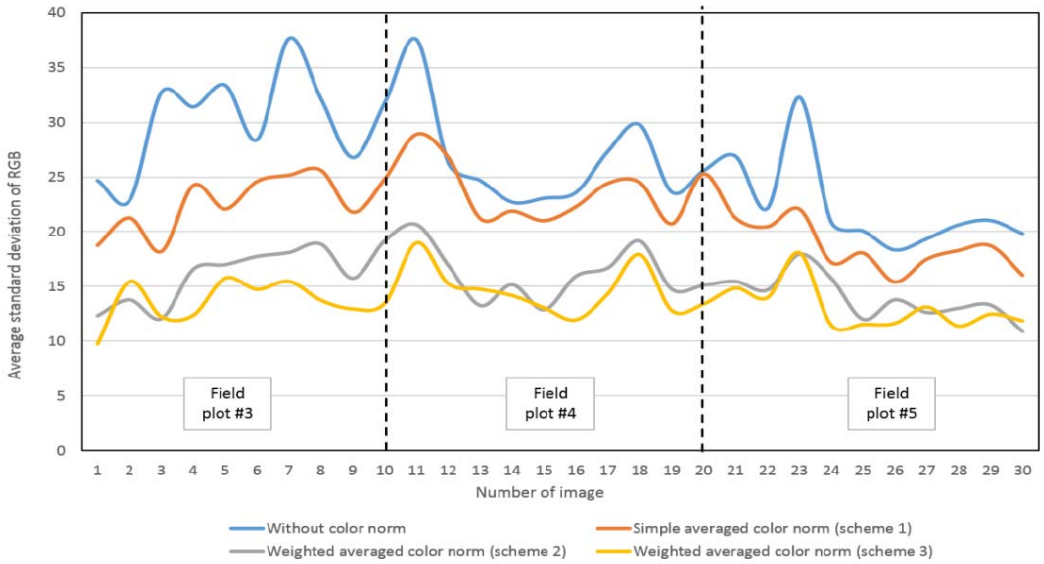

Figure 2. Comparison of color normalization results with three different schemes.

By applying the developed color normalization using scheme 1, i.e. simple average combiner, the standard deviation value, which is used as the parameter of color variability, can be decreased significantly. However, the developed GA-based weighted average combiner can reduce the color variability more effectively than the simple average method. This result indicates that each element in the matrix α has different influence factor to each DL-MLP in the color normalization step. In addition, the effect of the local-optimized matrix α to reduce the color variability of wheat plant images is not quite different compared to that of the global-optimized matrix α. In general, the global optimization (scheme #3), however, can reduce the average standard deviation of RGB color values slightly more than the local optimization (scheme #2).

The developed DL-MLP based image segmentation has successfully distinguished the wheat plants from complex background, such as soil, stones, weeds, and other undesirable images. As

seen in Figure 3, the original wheat plants images (a) are firstly normalized using the developed fusion of DL-MLPs as shown in figures (b). After normalization, the wheat plants are then segmented and transformed into binary images (c) by means of DL-MLP based image segmentation. Noise is subsequently removed by selecting the largest part of the images (d). The final step is putting back the RGB color of the largest part of the wheat leaves.

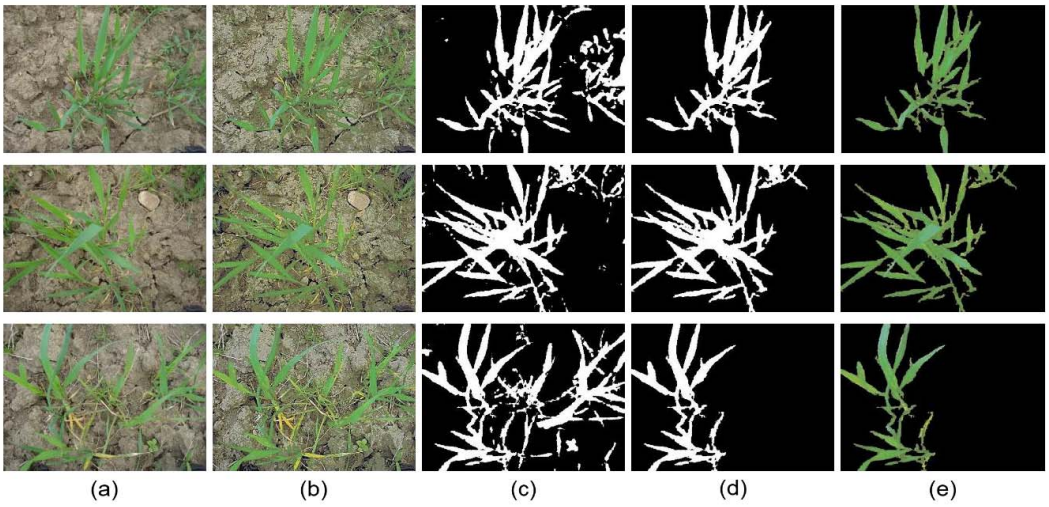

Figure 3. Examples of DL-MLP based image segmentation results.

The proposed global optimization is used to estimate nitrogen content in wheat leaves. Figure 4 shows the nitrogen estimation error is 0.0578, according to the SPAD meter. The first developed research scheme with a simple average combiner gave estimation results better than the SPAD meter based estimation. The best result based on this first scheme was obtained when using 7 MLPs in the nitrogen estimation step. On the other hand, in the second and third scheme, the best result was achieved from 6 MLPs. This finding indicates that GA-based color normalization gives some effects to the extracted statistical color features which were used as the inputs in the nutrient estimation step. Furthermore, the estimation results using 6 MLPs in the third scheme were slightly better than that in the second scheme. This point denotes that each MLP in the nitrogen estimation step has different weights (v) as a result of the developed GA. Based on our experiments, the best estimation results can be achieved by using the following formula:

$$N' = \sum_{q=1}^{6} \left(v_q \times N_q \right)$$

$$N' = \begin{bmatrix} 0.427 & 0.055 & 0.114 & 0.094 & 0.023 & 0.287 \end{bmatrix} \cdot \begin{bmatrix} N_1 \\ N_2 \\ N_3 \\ N_4 \\ N_5 \\ N_6 \end{bmatrix} \tag{23}$$

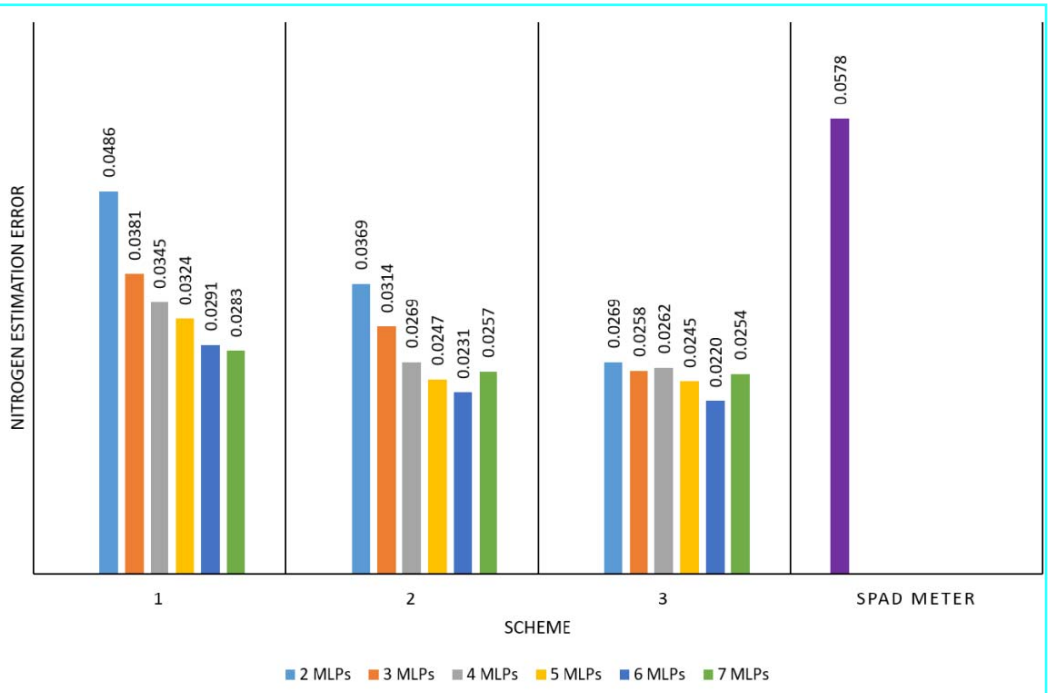

Figure 4. Nitrogen estimation error using three different schemes.

CONCLUSION

The variation of sunlight intensities will dominantly affect the color of wheat plant images. Therefore, color normalization is required to tackle the effect of differing sunlight intensity by reducing the color variability of the images. The proposed method focuses on global optimization using a genetic algorithm to normalize plant images that are subject to a variation in lighting conditions in order to estimate nitrogen content in wheat leaves. The globally optimized deep neural networks fusion has given the best prediction results compared to the other developed methods without global optimization and the common SPAD meter based estimation.

REFERENCES

1. S. Ivanov, K. Bhargava, and W. Donnelly, “Precision farming: sensor analytics,” IEEE Intelligent Systems, vol. 30, no. 4, 2015, pp. 76–80.
2. X. Yuanfang et al., “Study of monitoring maize leaf nutrition based on image processing and spectral analysis,” Proc. of IEEE World Autom. Congress (WAC), 2010, pp. 465–468.
3. S.B. Sulistyo, W.L. Woo, and S.S. Dlay, “Computational intelligent color normalization for wheat plant images to support precision farming,” Proc. of 8th IEEE Int. Conf. on Adv. Comput. Intell., 2016, pp. 130–135.
4. O. Abdel-Hamid et al., “Convolutional neural networks for speech recognition,” IEEE/ACM Trans. Audio, Speech, Lang. Process., vol. 22, no. 10, 2014, pp. 1533–1545.
5. Y. Wang et al., “Optimal formation of multirobot systems based on a recurrent neural network,” IEEE Trans. Neural Netw. Learn. Syst., vol. 27, no. 2, 2016, pp. 322–333.
6. P. Auearunyawat et al., “An automatic nitrogen estimation method in sugarcane leaves using image processing techniques,” Proc. of Int. Conf. on Agric., Environ. and Biological Sci. (ICAEBS), 2012, pp. 39–42.

7. H. Wang and D. Yeung, "Towards bayesian deep learning: a framework and some existing methods," IEEE Trans. on Knowl. Data Eng., vol. 28, no. 12, 2016, pp. 3395–3408.
8. Neuroshell 2, Ward System Group, 1998; http://www.wardsystems.com/manuals/neuroshell2/index.html?idxtutorialone.htm.
9. S.K. Ambat, S. Chatterjee, and K.V.S. Hari, "A committee machine approach for compressed sensing signal reconstruction," IEEE Trans. Sign. Process., vol. 62, no. 7, 2014, pp. 1705–1717.
10. A. Süß et al., "Measuring leaf chlorophyll content with the Konica Minolta SPAD-502Plus," EnMAP Field Guides Technical Report, technical report, GFZ Data Services, 2015.

ABOUT THE AUTHORS

Susanto B. Sulistyo is currently a PhD candidate with Newcastle University, UK. His major research area is in computational intelligent signal and image processing. He received his M.Sc. degree in Agricultural Engineering Sciences from Bogor Agricultural University, Indonesia.

W. L. Woo is currently a Reader in Intelligent Signal Processing with Newcastle University, UK. His major research area is in mathematical theory and algorithms for nonlinear signal and image processing. He received his PhD from Newcastle University in the areas of higher order statistics and machine learning. Dr Woo is a Senior Member of the IEEE.

S. S. Dlay is currently Professor of Signal Processing Analysis with Newcastle University, UK. His major research is in image processing ranging from biometrics to biomedical diagnosis. He received his PhD degree from the same institution in the area of signal processing architectures.

Bin Gao is currently Professor of Nondestructive Testing with University of Electronic Science and Technology of China. His major research is in signal processing for NDT. He received his PhD from Newcastle University, UK in the area of signal processing.